Available online at www.sciencedirect.com
ScienceDirect
Acta Materialia 58 (2010) 2207–2215
Acta MATERIALIA
www.elsevier.com/locate/actamat

An optimization-based computational model for domain evolution in polycrystalline ferroelastics

F.X. Li [a,b,*], A.K. Soh [c,1]

[a] State Key Lab for Turbulence and Complex Systems, College of Engineering, Peking University, Beijing 100871, China
[b] Center for Applied Physics and Technologies, Peking University, Beijing, China
[c] Department of Mechanical Engineering, The University of Hong Kong, Hong Kong, China

Received 21 October 2009; received in revised form 4 December 2009; accepted 4 December 2009
Available online 5 January 2010

Abstract

An optimization-based computational model is proposed to study domain evolution in polycrystalline ferroelastics composed of numerous randomly oriented grains, each of which consists of multiple types of domains. Under any prescribed loading, the volume fraction of each domain in a grain is obtained by minimizing the free energy of the said grain using an optimization method. The mechanical constraint from the neighboring grains is considered using Eshelby inclusion approach. This model has the similar superiority as the phase field model, which does not require imposition of any priori domain-switching criterion. The computational efficiency of this model is fairly high and it is feasible to study three-dimensional cases using numerous grains. Furthermore, this model can reproduce Taylor's rule of plasticity very well. Simulation results for tetragonal, rhombohedral and morphotropic PZT ceramics are employed to validate the superiority and efficiency of this model. The domain texture evolution process can also be calculated.

Keywords: Ferroelastics; Polycrystalline; Domain switching; Optimization; Plasticity

1. Introduction

Ferroelastics, including shape memory alloys (SMA), ferroelectrics and ferromagnetics, are materials in which multi-variants or multi-domains (each having a distinct spontaneous strain) exist below a certain temperature (Curie temperature or phase transformation temperature) and these domains can be reoriented by applied stress. In shape memory alloys [1], the ferroelastic properties are exhibited in the form of martensitic–austenitic phase transformations and reorientations of martensitic variants under applied stress. The shape memory effect is actually generated by the ferroelastic properties, although we usually do not use the terminology "ferroelastics" in SMA. In other material systems, such as ferroelectrics and ferromagnetics, the ferroelastic properties are usually associated with ferroelectricity or ferromagnetism, thus sometimes it may be deemed as a secondary effect. It should be noted that, even in ferroelectrics or ferromagnetics, the ferroelastic properties can also exist independently and appear with no ferroelectric or ferromagnetic effects, such as in the cases of a ferroelectric/ferromagnetic under applied stress. The ferroelastic properties are very useful in modern industries because of the well-known shape memory effect in SMA. Besides, as the ferroelastic properties are directly related to strain variations in materials, they are quite important in various actuator applications.

A ferroelastic material will show linear elastic properties at a low stress, but will exhibit intensive nonlinear stress–strain properties under a high stress, which is very similar to the case of plasticity. It should be mentioned that the

* Corresponding author. Address: Center for Applied Physics and Technologies, Peking University, Beijing, China. Tel.: +86 10 62757454; fax: +86 10 62751812.
E-mail addresses: lifaxin@pku.edu.cn (F.X. Li), aksoh@hkucc.hku.hk (A.K. Soh).
[1] Tel.: +852 28598061.

1359-6454/$36.00
doi:10.1016/j.actamat.2009.12.006

ferroelastic property is different from plasticity as the nonlinear strain in the former is due to domain reorientation (or domain switching), whereas it arises from dislocation slip in the latter. The nonlinear strain caused by domain switching in ferroelastics can usually be recovered by subsequent applied stress or by heating the material above the phase transformation temperature. However, the plastic strain caused by dislocation slips is generally irrecoverable.

While ferroelastics have hardly been studied independently, modeling of domain switching in ferroelectrics has received much attention in recent years [2–11]. Of the models, phase field modeling [6–11] seems most promising, as it does not require imposition of any priori domain-switching criterion, and domain switching is a natural process during minimization of the whole material system's total free energy. Although the phase field method (PFM) has achieved great success in modeling domain evolution in ferroelectric single crystals, it has hardly been used to study polycrystalline ferroelectrics [7,10,11], probably because of the difficulties encountered in addressing the complicated interactions, especially the elastic interactions between grains. The rather sizeable computational complexity encountered in handling three-dimensional (3-D) cases may be another challenge for the use of PFM.

In single-crystal ferroelastics, domain switching is relatively easy to accomplish, thus a single domain state can exist. However, the same cannot be said for polycrystalline ferroelastics because of the mechanical constraints from neighboring grains. Domain switching in ferroelastics is dependent on crystal symmetry, as is the resultant nonlinear recoverable strain. The nonlinear recoverable strain in SMA of various crystal symmetries have been systematically studied by Bhattacharya and Kohn [12], for both single crystals and polycrystals. It should be noted that in their work the recoverable strain in polycrystalline SMA was estimated using the Taylor bound; thus, only the lower limit was provided. The elastic interactions between grains were also crystal symmetry dependent. In our recent study [13], domain switching in both tetragonal and rhombohedral ferroelectric ceramics has been addressed by an analytical, constrained domain switching model, taking into account the interactions between grains by employing the Eshelby inclusion method. Note that in that model, an a priori domain-switching criterion and switching path must be prescribed and only uniaxial loading is allowed to obtain an analytical solution. Thus, the model is not suitable for a general computational study of domain evolution in polycrystallines under arbitrary loading. More recently, Tang et al. [14] studied crystal-symmetry-dependent domain switching in tetragonal, rhombohedral and ferroelectric ceramics near the morphotropic phase boundary (MPB) using the Monte Carlo method, with the interactions between grains considered also using the Eshelby inclusion method. In their work, a probabilistic switching criterion was used instead of the conventional inequality type of switching criterion employed by Hwang et al. [15]. As the computational complexity of the Monte Carlo method increases dramatically with the number of grains modeled, they used only 100 grains in their calculations [14].

In this work, we propose an optimization-based computational model to study the domain evolution process in polycrystalline ferroelastics of arbitrary crystal symmetries under arbitrary stress loading. In this model, a polycrystalline ferroelastic is composed of numerous randomly oriented grains, each of which consists of N types of domains ($N = 3$ for tetragonal, $N = 4$ for rhombohedral, etc.). The total free energy of each grain is set as the optimization objective using the volume fractions of different types of domains as the optimization variables. The optimization process is realized by the complex method proposed by Box [16], which is very efficient for solving constrained nonlinear optimization problems. Similar to the phase field model, this computational model also does not require imposition of any priori domain-switching criterion. Meanwhile, the computational complexity of this proposed model is fairly small compared to the PFM or the Monte Carlo method, thus it is feasible to study 3-D cases, in which numerous grains are modeled. Simulation results obtained from this model for tetragonal, rhombohedral and MPB ferroelectric ceramics tally well with those of the existing experiments. The model can also reproduce Taylor's rule of plasticity [17] very well. Furthermore, the domain texture evolution process can be explicitly calculated and presented step by step.

2. Material model

In the present study, a polycrystalline ferroelastic material is deemed to consist of numerous randomly oriented grains, each of which contains N types of domains (where $N = 3$ for the tetragonal, $N = 4$ for the rhombohedral, $N = 6$ for the orthorhombic, etc.). The volume fraction of each type of domains is denoted by f_i $(i = 1, 2 \ldots N)$ and $\sum_{i=1}^{N} f_i = 1$. During domain switching, the elastic interactions between the grains are assumed to be in a self-consistent inclusion manner [18]. This is to say, each grain is regarded as an inclusion surrounded by an infinitely large matrix with material properties the same as the bulk, as shown in Fig. 1, which is a 2-D model. As spherical inclusion is the simplest one, and there is no evidence to suggest that other shapes of inclusion are more accurate, so this type of inclusion was employed to devise this model.

For single-crystal ferroelectrics or SMA, the main concern of researchers may be the domain patterns (or martens-

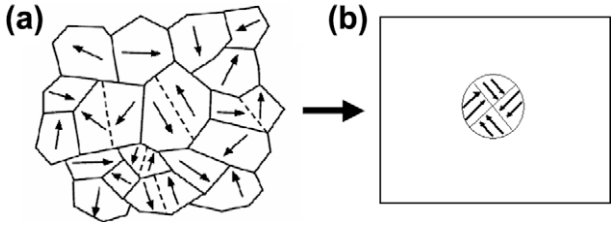

Fig. 1. 2-D illustration of the model of a polycrystalline ferroelastic material.

ite patterns) as they have strong influences on the material properties. In dealing with polycrystals, the detailed topological structures of domains in a specific grain are normally insignificant as the material consists of numerous grains usually oriented in all directions. In the present study, the concept of a "topology-insensitive structure" is introduced in the model, which means that the domain structure inside a grain can only be determined by the volume fraction of different types of domains and is independent of the detailed topological relations between them. In other words, if there are two domain structures which have the same volume fraction of domains but different topological relations, such domain structures are taken to be the same. The topology-insensitive structure of domains thus becomes the domain texture, and is expressed by the pole figure of the elongation axis of domains in this paper.

Furthermore, to grasp the main characteristics of domain switching and to make the computational complexity manageable, we further assume that a ferroelastic polycrystalline is elastically isotropic and exhibits linear elastic behavior unless domain switching occurs (i.e. all the nonlinear strains are caused by domain switching).

3. Free energy of a single grain

In this model, the free energy of each grain is taken as the optimization objective and the optimization process is repeated over all grains to determine the volume fractions of domains, the domain textures and resultant strains of the whole material system at each step of loading. The free energy of a specific grain is expressed as

$$\begin{aligned} U(\boldsymbol{\sigma},\boldsymbol{\varepsilon}^r,\bar{\boldsymbol{\varepsilon}}) &= -\boldsymbol{\sigma}:\boldsymbol{\varepsilon}^r + \frac{1}{2}\frac{1}{2\mu(1+v)}\boldsymbol{\sigma} \\ &: \boldsymbol{\sigma} + \frac{1}{2}\cdot 2\mu\frac{7-5v}{15(1-v)}(\boldsymbol{\varepsilon}^r-\bar{\boldsymbol{\varepsilon}}) \\ &: (\boldsymbol{\varepsilon}^r-\bar{\boldsymbol{\varepsilon}}) + f_{sw}\cdot W_{sw} \end{aligned} \tag{1}$$

where U, $\boldsymbol{\sigma}$, $\boldsymbol{\varepsilon}^r$ and $\bar{\boldsymbol{\varepsilon}}$ are the free energy of the specific grain, applied stress, remnant strain of the specific grain and average remnant strain of the whole material system, respectively; μ, v are the isotropic shear moduli and Possion ratio, respectively; and W_{sw} and f_{sw} are the energy barrier (per unit volume) and the accumulative volume fraction of ferroelastic domain switching, respectively.

The energy barriers for all types of ferroelastics switching in single-phase materials can be expressed in an united form as $W_{sw} = S_0\sigma_C$, where S_0 is the single-crystal deformation given by $S_0 = S_{lattice} = c/a - 1$ for the tetragonal crystal (c, a are the tetragonal lattice constants) and $(8/9)S_0 = S_{lattice} = d_{[1\,1\,1]}/d_{[1\,1\,\bar{1}]} - 1$ for the rhombohedral crystal ($d_{[1\,1\,1]}, d_{[1\,1\,\bar{1}]}$ are the rhombohedral lattice constants) [13]; σ_C is the nominal coercive stress. For the case of polycrystalline ferroelastics near MPB (where tetragonal phase and rhombohedral phase coexists) to be addressed in this paper, the energy barriers for both the in-phase and inter-phase ferroelastic domain switching are taken to be the same values as those of the rhombohedral ferroelastics.

At each step of loading, the accumulative volume fraction of ferroelastic switching, i.e. f_{sw} in Eq. (1), can be calculated using the volume fractions of domains before and after domain switching as follows:

$$f_{sw} = \frac{1}{2}\sum_{i=1}^{N}|f_i - f_i^0| \tag{2}$$

where f_i $(i = 1,\ldots,N)$ is the volume fraction of the ith domain after current switching, which is solved by the optimization process, and f_i^0 is the volume fraction of the ith domain before current switching, obtained at the previous loading step.

In Eq. (1), the remnant strain of a specific grain, i.e. $\boldsymbol{\varepsilon}^r$, can be expressed by a linear function of the volume fractions of domains as follows:

$$\boldsymbol{\varepsilon}^r = \sum_{i=1}^{N} f_i\boldsymbol{\varepsilon}^i \tag{3}$$

where $\boldsymbol{\varepsilon}^i$ is the spontaneous strain tensor of the ith domain. The three types of domains in the tetragonal ferroelastics and the four types in the rhombohderal ferroelastics can be depicted in the cubic crystallite coordinates, as shown in Fig. 2a and b, respectively.

The corresponding spontaneous strain tensors for the tetragonal domains are:

$$\begin{aligned} \boldsymbol{\varepsilon}^{\mathrm{T1}} &= \frac{S_0^T}{3}\begin{bmatrix} -1 & & \\ & -1 & \\ & & 2 \end{bmatrix}, \quad \boldsymbol{\varepsilon}^{\mathrm{T2}} = \frac{S_0^T}{3}\begin{bmatrix} 2 & & \\ & -1 & \\ & & -1 \end{bmatrix}, \\ \boldsymbol{\varepsilon}^{\mathrm{T3}} &= \frac{S_0^T}{3}\begin{bmatrix} -1 & & \\ & 2 & \\ & & -1 \end{bmatrix} \end{aligned} \tag{4}$$

where $\boldsymbol{\varepsilon}^{\mathrm{Ti}}$ $(i = 1,2,3)$ is the spontaneous strain tensor of the ith tetragonal domain and S_0^T is the single-crystal deformation of tetragonal ferroelastics.

The spontaneous strain tensors for the rhombohedral domains are

$$\begin{aligned} \boldsymbol{\varepsilon}^{\mathrm{R1}} &= \frac{S_0^R}{3}\begin{bmatrix} 0 & 1 & 1 \\ & 0 & 1 \\ sym & & 0 \end{bmatrix}, \quad \boldsymbol{\varepsilon}^{\mathrm{R2}} = \frac{S_0^R}{3}\begin{bmatrix} 0 & -1 & 1 \\ & 0 & -1 \\ sym & & 0 \end{bmatrix}, \\ \boldsymbol{\varepsilon}^{\mathrm{R3}} &= \frac{S_0^R}{3}\begin{bmatrix} 0 & -1 & -1 \\ & 0 & 1 \\ sym & & 0 \end{bmatrix}, \quad \boldsymbol{\varepsilon}^{\mathrm{R4}} = \frac{S_0^R}{3}\begin{bmatrix} 0 & 1 & -1 \\ & 0 & -1 \\ sym & & 0 \end{bmatrix} \end{aligned} \tag{5}$$

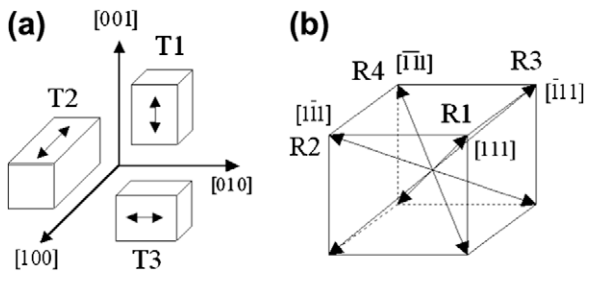

Fig. 2. Different types of domains in (a) tetragonal and (b) rhombohderal ferroelastics.

Table 1
Material constants of the tetragonal, rhombohedral and morphotropic PZT ceramics used in the model.

Material constants	Rhombohedral	Tetragonal
Shear modulus, μ (GPa)	30	
Poisson's ratio, v	0.3	
Single-crystal deformation, S_0 in single-phase PZT ceramics	0.73%	2.77%
Single-crystal deformation in morphotropic PZT ceramics	1.0%	2.0%
Nominal coercive stress, σ_C (MPa)	70	

where $\boldsymbol{\varepsilon}^{\mathrm{Ri}}$ $(i = 1, 2, 3)$ is the spontaneous strain tensor of the ith rhombohedral domain and S_0^R is the single-crystal deformation of rhombohedral ferroelastics.

Referring to the expression of the free energy in Eq. (1), the first to fourth items on the right-hand side are the potential energy [15], linear elastic strain energy, inclusion strain energy or misfit strain energy and dissipation energy for domain switching (which is similar to the domain wall energy in phase field models [6]), respectively.

4. Optimization methodology

As mentioned above, in the proposed model the volume fraction of each type of domains in a specific grain, i.e. f_i, is obtained by minimizing the free energy U of the whole grain via an optimization process. At each step of loading, the mathematical optimization problem for a specific grain can be abstracted as Problem I:

$$\begin{aligned} &\text{Min} \quad U(f_1, f_2, \cdots, f_N) \\ &s.t. \quad 0 \leqslant f_i \leqslant 1 \quad (i = 1, 2, \cdots, N) \\ &\qquad \sum_{i=1}^{N} f_i = 1 \end{aligned} \tag{6}$$

It can be seen from Eqs. (1)–(5) that the free energy U is a nonlinear function of the volume fractions of domains. Thus, Eq. (6) turns out to be a constrained nonlinear optimization problem, which can be solved using the complex method proposed by Box [16], in which a very effective algorithm with high accuracy and quick convergence is implemented. As the expression of the free energy varies from grain to grain and depends on the applied loading, at each step of loading the optimization process is repeated over all grains, and the volume fractions of domains, domain textures and switching strains are calculated.

5. Results and discussion

In the present study, both tetragonal and rhombohdral single-phase PZT ceramics and PZT ceramics near the MPB (also called morphotropic PZT) under uniaxial compression/tension are calculated using the proposed computational model. The materials constants used in the simulations are listed in Table 1, which are taken from Hoffmann et al. [19] with slight modifications made because of the isotropic elastic assumptions. For a better comparison, the elastic properties and the nominal coercive stress of all types of ceramics are taken to be the same as they do not differ much in reality. It should be noted that in Table 1 the single-crystal deformations in single-phase tetragonal and rhombohedral PZT ceramics are different from those in the morphotropic PZT ceramics.

5.1. Convergence and computational complexity

The simulation results for all types of PZT ceramics have shown that strain–stress curves will stabilize only after 1.5 cycles of uniaxial tension–compression loading. The strain–stress curves for subsequent cyclic loading completely overlap the former curves, which indicate good convergence of this model.

By focusing on the volume fractions of domains instead of the detailed domain patterns in grains, this optimization-based model has a much smaller computational complexity compared to the phase field model, and it is thus feasible to study 3-D cases using a very large number of grains. For the case of a polycrystalline ferroelastic material with 10,000 grains and 61 loading steps, the computation time of this model on a Pentium 3.0 GHz PC is only 40 min for tetragonal PZT ceramics, about 8 h for rhombohedral PZT ceramics and 21 h for the morphotropic PZT ceramics.

5.2. Tetragonal PZT

Fig. 3 shows the switching strain vs. stress curves of tetragonal PZT ceramics under uniaxial tension and compression up to 350 MPa ($5\sigma_C$). It can be seen from Fig. 3 that the switching strain under tension and compression is symmetric and very small. The maximum switching strain in both cases is about 0.1% and the remnant strain is only about 0.04%. The switching strain is far from saturation even under a high stress ($5\sigma_C$), which indicates that ferroelastic domain switching in tetragonal PZT ceramics is very difficult to accomplish. These calculated results tally well with the experimental results on tetragonal PZT ceramics [20] and are also consistent with the small fractions of 90° domain switching in

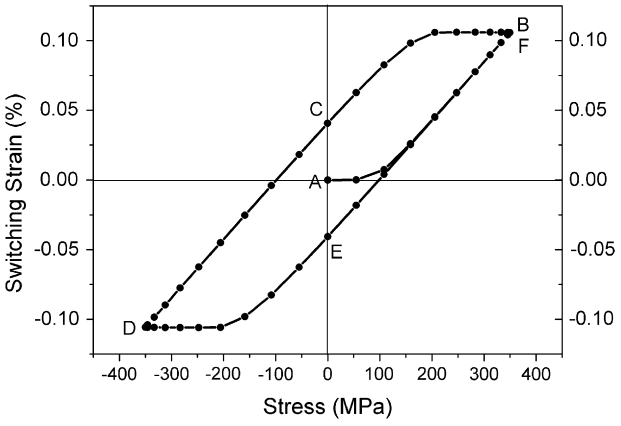

Fig. 3. Switching strain–stress curves of tetragonal PZT ceramics under uniaxial tension and compression.

$BaTiO_3$ ceramics under stress [21,22]. The simulation results under a very high tensile stress may be trivial as the tension strength of PZT ceramics is usually no more than 50 MPa [23]; these results are presented to show the tendency and make a comparison with the theoretical studies [24,25]. Furthermore, the model can be directly employed to study the case of SMA [1,12], the tension and compression strengths of which are usually comparable.

To show the process of domain texture evolution, the pole figure [26] of the elongation axis, i.e. (0 0 1) for the tetragonal grains, is calculated at each loading step. Under uniaxial compression or tension, the pole figure of the elongation axis is axisymmetric around the loading axis and can thus be described by an angular distribution function $g(\theta)$ $(0 \leqslant \theta \leqslant \pi/2)$ [25], where $g(\theta) \equiv 1$ for the random uniform distribution and the normalization condition requires

$$\int_0^{\pi/2} g(\theta) \sin\theta d\theta = 1 \tag{6}$$

From its definition, it can be seen that $g(\theta)$ completely depends on ferroelastic domain switching.

The mathematically saturated domain textures (where interactions between domains are neglected) of tetragonal and rhombohedral ferroelectric ceramics after complete mechanical poling by uniaxial tension and compression has been analytically derived previously [25] and is replotted in Fig. 4. The saturated domain textures for MPB ferroelectric ceramics, however, are absent.

In the present study, $g(\theta)$ is calculated using 10,000 grains and the interval of [0°, 90°] is divided into 18 subintervals giving rise to equal interval of 5°. The accumulated volume fractions of domains at all these subintervals give the values of $g(\theta)$ at discrete values of θ, which are midpoints of the 18 subintervals.

Fig. 5 shows the calculated pole figure of (0 0 1) axis in tetragonal PZT ceramics under different loading steps, as

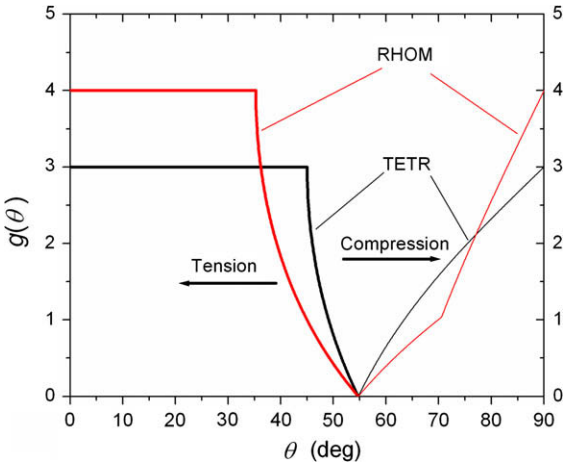

Fig. 4. Mathematically saturated pole figures of elongation axis for tetragonal (TETR) and rhombohedral (RHOM) ferroelectric ceramics after complete mechanical poling by uniaxial tension and compression [25].

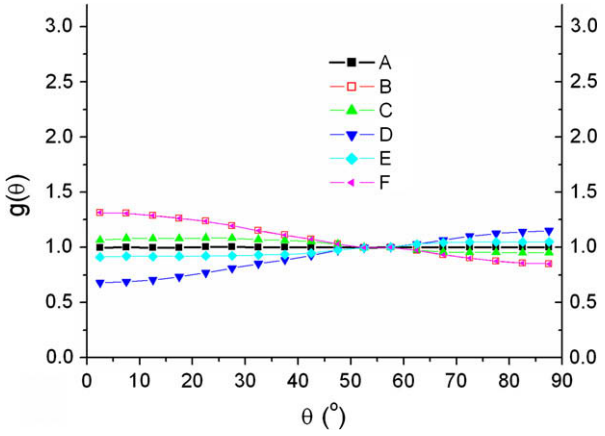

Fig. 5. (0 0 1) pole figures of tetragonal PZT ceramics under uniaxial tension and compression.

illustrated in Fig. 3. For convenience, in both Figs. 3 and 5, states A, B, C, D, E and F are called initial state, tension saturated state, tension remnant state, compression saturated state, compression remnant state and repeated tension saturated state, respectively. It can be seen from Fig. 5 that, compared to the initial random state A, the domain textures at the saturated states (B, D and F), where the maximum stress is attained, change to some extent but are still far from the saturated domain texture, as shown in Fig. 4 [25]. The remnant domain textures at states C and E do not change much from the initial state A, which tallies well with the little remnant strain shown in Fig. 3. The symmetric domain textures under tension and compression, as shown in Fig. 5, are also consistent with the symmetric switching strains presented in Fig. 3.

5.3. Rhombohedral PZT

Fig. 6 shows the switching strain vs. stress curve and (1 1 1) pole figures of rhombohedral PZT ceramics under uniaxial tension and compression up to 350 MPa. It can be seen from Fig. 6a that, quite different from the case of tetragonal PZT ceramics, a considerable amount of switching strains can be realized in rhombohedral PZT ceramics via ferroelastic domain switching. Moreover, the switching strains under uniaxial tension and compression are not symmetric. The positive switching strain under maximum tension is about 0.25%, while the negative strain under maximum compression is only about −0.16%. The asymmetric deformation of ferroelastic materials under tension and compression is due to the asymmetric spontaneous strain of ferroelastic domains, which is $2S_0/3$ for elongation and $-S_0/3$ for contraction. The asymmetry of mathematical saturated strains under uniaxial tension and compression has already been discovered [24,25,27]. Since the switching strains under maximum stress in Fig. 6a are approaching the mathematical saturated values (0.31% under tension and −0.21% under compression) [25], they should share the similar asymmetric properties of the

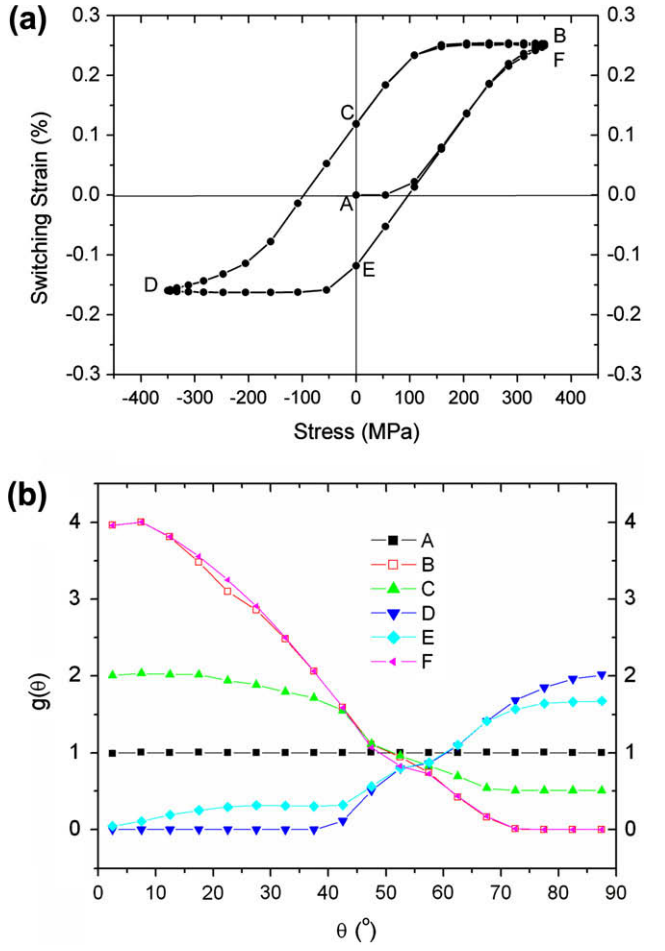

Fig. 6. (a) Switching strain–stress curve and (b) (1 1 1) pole figures of rhombohedral PZT ceramics under uniaxial tension and compression.

mathematical saturated strains. However, in Fig. 6a, the remnant strains under tension and compression are almost the same, at about 0.12%.

The calculated pole figures of elongation axis in rhombohedral PZT ceramics, as shown in Fig. 6b, are also quite different from those of tetragonal PZT ceramics, as shown in Fig. 5. In fact, the domain textures of rhombohedral PZT ceramics change a lot from its initial unpoled state. Under uniaxial tension, most domains switch to a state where the elongation axis forms a very acute angle ($\theta < 55°$) with the tension direction. By comparing Fig. 6b with the mathematical saturated domain textures shown in Fig. 4, it can be seen that the (1 1 1) pole figure $g(\theta)$ at the tension saturated state B and the repeated tension saturated state F is approaching the saturated pole figure shown in Fig. 4. After removing the tensile stress, some fractions of back switching occurs, as can be clearly seen from the domain texture evolution from state B to state C. Under maximum uniaxial compression, most domains switch to a state where its elongation axis forms a large angle ($\theta > 55°$) with the compressive direction. Unlike the case of maximum tension (states B and F), the domain textures at maximum compression (state D), as shown in Fig. 6b, are obviously not as close to the mathematical saturated textures shown in Fig. 4. Upon removing the compressive stress, the domain texture at state E does not change much from that at the compression saturated state D, indicating that little back ferroelastic switching occurs, which is consistent with the small strain variations from point D to point E, as shown in Fig. 6a. Anyway, in rhombohedral PZT ceramics, after a high uniaxial tension or compression, the domain textures approach the theoretical saturated states [25] and cannot return to the initial state in subsequent loading.

5.4. Morphotropic PZT

Further calculations are carried out for the domain evolution in PZT ceramics near the MPB where tetragonal and rhombohedral phases coexist. In the simulation we assume that the morphotropic PZT ceramics contain equal fractions of tetragonal and rhombohedral phases. Fig. 7 shows the simulated switching strain–stress curves and the cumulative pole figures of (0 0 1) and (1 1 1) axes in morphotropic PZT ceramics under uniaxial tension and compression. It can be seen from Fig. 7a that, similar with the rhombohe-

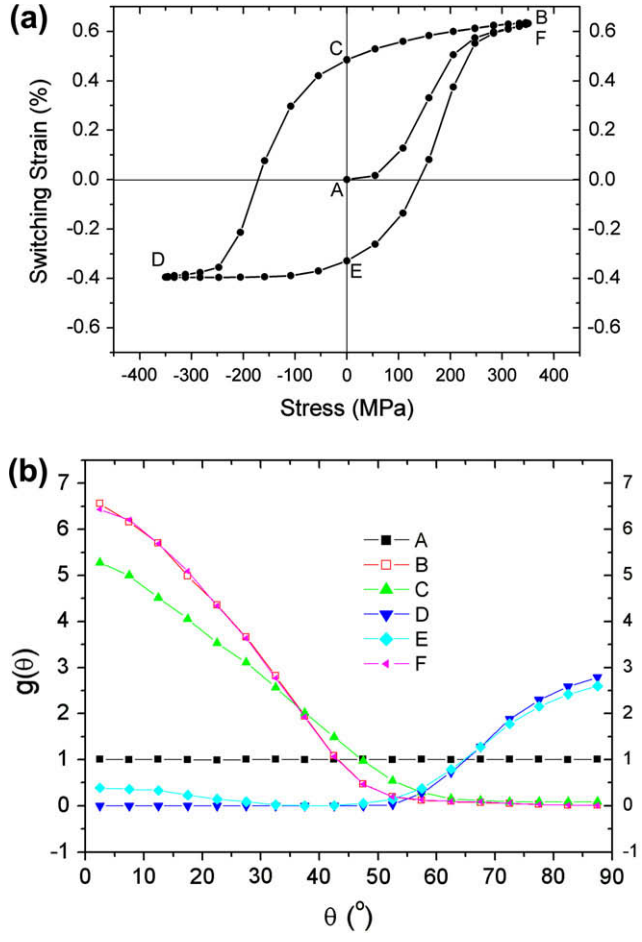

Fig. 7. (a) Switching strain–stress curves and (b) the cumulative pole figures of the (0 0 1) and (1 1 1) axes in morphotropic PZT ceramics under uniaxial tension and compression.

dral PZT case shown in Fig. 6a, the switching strain under maximum tension (about 0.62%) is considerably larger than that under maximum compression (0.4%). However, different from that shown in Fig. 6a, the remnant switching strain under tension (about 0.5%) is also larger than that under compression (about 0.35%). The calculated remnant strain under compression (0.35%) is very close to the few experimental data obtained very recently, i.e. 0.3% [28] and 0.33% [29], on unpoled morphotropic PZT ceramics under compression. The back ferroelastic switching that occurs in morphotrpic PZT ceramics upon removing the applied stress is not as obvious as that of the rhombohedral and tetragonal PZT ceramics. Note that over 80% of maximum switching strain is retained in morphotropic PZT ceramics, as shown in Fig. 7a, while the corresponding value is only about 40% for tetragonal PZT and 48% for rhombohedral PZT, as shown in Figs. 3 and 6a, which may indicate that the internal stress caused by ferroelastic switching in morphotropic PZT ceramics is not very large.

The domain textures of morphotropic PZT ceramics under applied stress, as shown in Fig. 7b, shows that under maximum tension at states B and F, as expected, most domains switch to a state where their elongation axis is oriented as close as possible to the tensile direction. Within the narrow range of $\theta < 10°$, $g(\theta)$ reaches a value higher than 6, which is approaching the mathematical saturated value of 7. After removing the uniaxial tension, some domains return to their initial states, making curve C slightly lower than curve B within a small range of θ (say $\theta < 30°$). Under maximum uniaxial compression, most domains switch to a state where their elongation axis is oriented as perpendicular as possible to the compression direction (see state D in Fig. 7b), where $g(\theta)$ vanishes from $\theta = 0°$ to $\theta \approx 55°$, after which it increases gradually with θ. The maximum value of $g(\theta)$ at 90° is only about 3, which is considerably smaller than the mathematical saturated value of 7. This may be an indication that it is more difficult to reach the saturated domain orientation state under uniaxial compression than under uniaxial tension. The almost overlapped curves at states D and E, as shown in Fig. 7b, shows that only a little back ferroelastic switching occurs upon removing the compressive stress, which is consistent with the small strain variations between points E and D shown in Fig. 7a.

5.5. Reproduction of Taylor's rule of plasticity

It can be seen from Figs. 3, 6a and 7a that the remnant switching strain of the morphotropic PZT ceramics (0.5% under tension and 0.35% under compression) is much larger than that of the tetragonal (0.04%) and rhombohedral PZT ceramics (0.12%). This tendency can be seen more clearly in Fig. 8, where the switching strain vs. stress curves for three types of PZT ceramics are replotted for comparison. The remnant strain in polycrystalline ferroelastics is crystal symmetry dependent. According to Taylor's rule of plasticity [17], a crystal must have at least five slip systems for its polycrystalline to be ductile. In terms of the

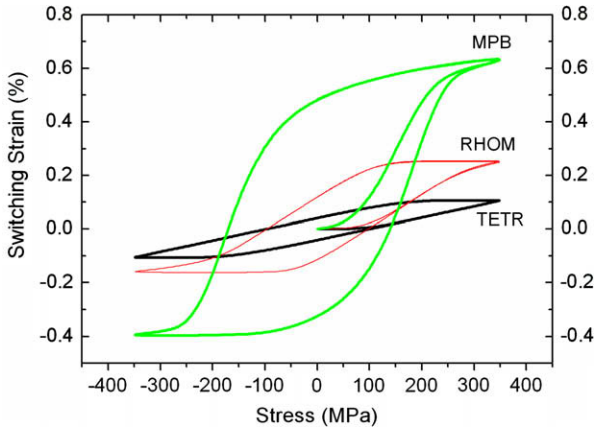

Fig. 8. Comparison of switching strain vs. stress curves of tetragonal, rhombohedral and MPB PZT ceramics (the nominal coercive stress $\sigma_C = 70$ MPa).

deformation modes, a tetragonal ferroelastic crystal has three slip systems (two of which are independent) and a rhombohedral ferroelastic crystal has four (three of which are independent). Thus, in tetragonal or rhombohedral polycrystalline ferroelastics, the change in spontaneous strain in a particular grain during ferroelastic domain switching cannot be accommodated by neighboring grains and will therefore generate large internal stresses inside the grain, i.e. such ferroelastic switching will be constrained by the surrounding grains and may not occur. The tetragonal and rhombohedral PZT ceramics are thus brittle materials from this point of view. In PZT ceramics near the MPB, where tetragonal and rhombohedral phases coexist, there are a total of six independent deformation modes, which causes the material to be ductile. During ferroelastic switching in morphotropic PZT ceramics, most of the switching strains in a particular grain can be accommodated by neighboring grains. Thus, the ferroelastic domain switching does not generate very large internal stress in the grain and can be almost completely accomplished in morphotropic PZT ceramics [20].

Based on Taylor's rule of plasticity, the remnant switching strain for tetragonal and rhombohedral PZT ceramics should be zero In fact, the nonzero simulated remnant strain in the tetragonal and rhombohedral PZT ceramics (refer to Fig. 8) is due to the large coercive stress (70 MPa) for ferroelastic domain switching. If a very small coercive stress (say 5 MPa) is employed for simulation, the remnant strain for both tetragonal and rhombohedral ceramics will reduce to nearly zero, leading to almost hysteresis-free strain–stress curves, as shown in Fig. 9. However, the remnant strain of the morphotropic PZT ceramics is still fairly large even if a small coercive stress is used, and it can be estimated from the Taylor bound [12], which gives the lower limit. The Taylor bound of remnant strain in morphotropic PZT ceramics is not yet available, but can also be calculated using the proposed model by just prescribing an infinitely large isotropic elastic modulus and a very small coercive stress. For the morphotropic

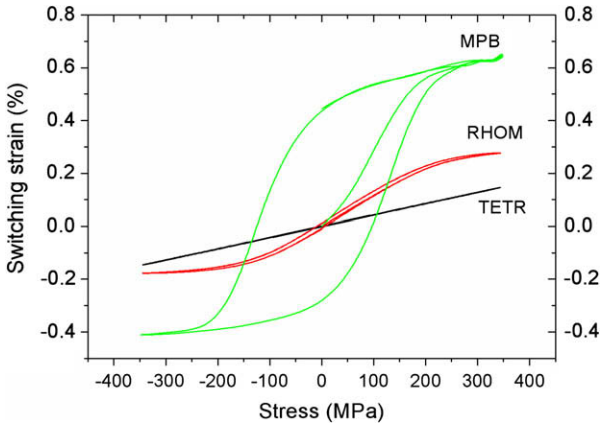

Fig. 9. Simulated switching strain vs. stress curves of tetragonal, rhombohedral and MPB PZT ceramics using a small nominal coercive stress of $\sigma_C = 5$ MPa.

PZT ceramics with the values of single-crystal deformation listed in Table 1, the Taylor bound of remnant switching strain is 0.32% under uniaxial tension and 0.22% under uniaxial compression, which, as expected, are smaller than the remnant strain in real cases (0.5% under uniaxial tension and 0.35% under uniaxial compression, as shown in Fig. 8). From both Figs. 8 and 9, we can thus conclude that the proposed model can reproduce Taylor's rule of plasticity very well.

It should be mentioned that the PZT ceramics used in the above simulations are actually both ferroelectrics and ferroelastics. Although pure ferroelectric (or 180°) domain switching may occur in these materials under electric fields, the scope of the present work only involves unpoled PZT ceramics under mechanical loading and, therefore, the said domain switching is not considered. During domain switching in an unpoled PZT ceramic under compression, domains will reorientate in a head-to-head or tail-to-tail manner to minimize the electric depolarization field energy. Thus, no net polarization will be produced in the material, as has been confirmed experimentally [28,29]. Unpoled PZT ceramics under mechanical loading can hence be treated as pure ferroelastic materials. However, this does not apply to poled PZT ceramics under compression, where domain switching is always accompanied by polarization variations [15,23,28–30]. The electrical poling has a permanent effect on a poled PZT ceramic which cannot be removed completely by stress alone [24,25].

6. Conclusions

In summary, an optimization-based computational model for domain evolution in polycrystalline ferroelastics is proposed. In the model, the free energy of each grain is taken as the optimization objective and the volume fraction of each domain type as the optimization variable. This model has similar advantages as the phase field model (PFM), i.e. it does not require imposition of any priori domain switching criteria or prescription of any switching paths, thus domain switching is a natural process of minimization of free energy in each grain. The computational complexity of this model is much smaller, and it is feasible to study domain evolution in polycrystalline ferroelastics for 3-D cases using a large number of grains. Similar to the case of PFM, where the domain patterns in single crystals can be calculated, the evolution process of domain textures in polycrystalline ferroelastics can be represented by this optimization model. Furthermore, the proposed model can reproduce Taylor's rule of plasticity very well. Simulation results on tetragonal, rhombohedral and morphotropic PZT ceramics show the superiority and efficiency of this model.

The proposed optimization-based computational model is a general model for predicting all types of polycrystalline ferroelastics without using any fitting parameters. It can also be extended to analyze domain evolutions in other polycrystalline ferroic materials, such as ferroelectrics, ferromagnetics and ferromagnetic FSMA, which are the subjects of our ongoing work. Furthermore, this model can be slightly modified to study the dislocation movements in polycrystalline elastic–plastic materials with multiple slip systems.

Acknowledgements

F.L. is grateful for the financial support from the National Natural Science Foundation (Grant No. 10872002) and the 985 Project Foundation of Peking University. Support from the Research Grants Council of the Hong Kong Special Administrative Region, China (Project Nos. HKU 716007E) is also acknowledged.

References

[1] Otsuka K, Ren X. Prog Mater Sci 2005;50:511.
[2] Huber JE, Fleck NA, Landis CM, McMeeking RM. J Mech Phys Solids 1999;47:1663.
[3] Landis CM. J Mech Phys Solids 2002;50:127.
[4] Li FX, Fang DN. Mech Mater 2004;36:959.
[5] Zhang W, Bhattacharya K. Acta Mater 2005;53:185.
[6] Chen LQ. Annu Rev Mater Res 2002;32:113.
[7] Wang YU, Jin YM, Khachaturyan AG. J Appl Phys 2002;92:1351.
[8] Wang J, Shi SQ, Chen LQ, Li YL, Zhang TY. Acta Mater 2004;52:749.
[9] Soh AK, Song YC, Ni Y. J Am Ceram Soc 2006;89:652.
[10] Choudhury S, Li YL, Krill III CE, Chen LQ. Acta Mater 2005;53:5313.
[11] Schrade D, Mueller R, Xu B, Gross D. Comput Methods Appl Mech Eng 2007;196:4365.
[12] Bhattacharya K, Kohn RV. Acta Mater 1996;44:529.
[13] Li FX, Rajapakse RKND. Acta Mater 2007;55(Part I):6472. Part II, 6481.
[14] Tang W, Fang DN, Li JY. J Mech Phys Solids 2009;57:1683.
[15] Hwang SC, Lynch CS, McMeeking RM. Acta Metall Mater 1995;43:2073.
[16] Box MJ. Comput J 1965;8:42.
[17] Taylor GI. J Instrum Met 1938;62:307.
[18] Eshelby JD. Proc Roy Soc Lond A 1957;241:376.
[19] Hoffmann MJ, Hammer M, Endriss A, Lupascu DC. Acta Mater 2001;49:1301.

[20] Li JY, Rogan RC, Üstündag E, Bhattacharya K. Nat Mater 2005;4:776.
[21] Subbarao EC, McQuarrie MC, Buessem WR. J Appl Phys 1957;28:1194.
[22] Berlincourt D, Krueger HHA. J Appl Phys 1959;30:1804.
[23] Fett T, Munz D. Adv Eng Mater 2003;5:718.
[24] Landis CM. J Appl Mech-T ASME 2003;70:470.
[25] Li FX, Rajapakse RKND. J Appl Phys 2007;101:054110.
[26] Bunge HJ. Texture analysis in materials science. Berlin: Butterworth; 1982.
[27] Li FX, Fang DN, Soh AK. Scripta Mater 2006;54:1241.
[28] Webber KG, Aulbach E, Key T, Marsilius M, Granzow T, Rödel J. Acta Mater 2009;57:4614.
[29] Li YW, Zhou XL, Li FX, submitted for publication.
[30] Li FX, Fang DN. Acta Mater 2005;53:2665.